

# Combustion Behavior and Thermophysical Properties of Metal-Based Solid Fuels

D. M. Chen,\* W. H. Hsieh,† T. S. Snyder,‡ V. Yang,§ T. A. Litzinger,§ and K. K. Kuo¶  
*Pennsylvania State University, University Park, Pennsylvania 16802*

Two metal-based solid fuels (magnesium-based and boron-based) have been studied to determine their combustion behavior and thermophysical properties. The burning rate for the magnesium-based (Mg/PTFE/Viton A) solid fuel was found to increase monotonically with ambient pressure and to follow the Saint Robert's law in both air and nitrogen environments. The fuel, however, burned 10% slower in air than in nitrogen. The slower burning rate in air is postulated to result from the entrained oxygen which competes with fluorine to react with magnesium. Because of the lower heat of formation of  $MgO$  vs  $MgF_2$ , the near-surface heat release is reduced when the oxygen is present, thus reducing the burning rate. This reasoning is also supported by results obtained from the companion pressure deflagration limit (PDL) and ignition tests, which show that the combustion of the magnesium-based fuel has a higher PDL and a longer ignition delay time in air than in nitrogen. Results from the study of ignition and combustion characteristics of boron-based solid fuels show that boron can significantly reduce the ignition delay times of poly(BAMO/NMMO). In determining the thermophysical properties of fuel samples, a subsurface temperature-measurement method was developed to quantify the temperature dependence of the thermal diffusivities of fuel samples. Results show good agreement with those obtained with the laser-flash method.

## Nomenclature

PDL	= pressure deflagration limit, kPa
$r_b$	= burning rate, mm/s
$p$	= pressure, kPa
$K$	= thermal conductivity, W/K-cm
$\rho_p$	= density, g/cm <sup>3</sup>
$C_p$	= specific heat, J/g-K
$\dot{q}_{sub}$	= net heat release from subsurface, W/g
$\alpha$	= thermal diffusivity cm <sup>2</sup> /s
$L$	= sample thickness, cm
$t_c$	= characteristic rise time, s
$\tau$	= laser pulse time, s
$t$	= time, s
$t_{1/2}$	= time to reach one-half of maximum value, s

## Introduction

IN the search for new and improved propulsion technology, the solid-fueled ramjet engine has become an attractive candidate because of its simplicity and high performance. Among the various solid fuels that are under consideration for ramjet use, the boron-based and magnesium-based fuels are the most promising because of the high volumetric heating value of boron and the high combustion efficiency of magnesium. However, the poor ignition behavior of boron particles usually leads to lower combustion efficiency, making them impractical for use in an actual system. On the other hand,

magnesium particles possess superior ignition behavior but offer considerably lower heat of reaction. Thus, methods of enhancing the combustion efficiency of boron and retaining the ignition characteristics of magnesium are essential in order to render these fuels feasible for propulsion applications.

Two types of solid fuels were considered. The first contained magnesium with polytetrafluoroethylene (PTFE) and vinylidene fluoride w/perfluoropropylene (Viton A). The second contained boron with a highly energetic binder, 3,3-bis (azidomethyl) oxetane/3-nitratomethyl 3-methyloxetane [poly-(BAMO/NMMO)]. To date, efforts to examine the fundamental ignition and combustion behavior of these fuels have been few. Peretz<sup>1</sup> studied various thermochemical properties of several metal/fluorocarbon fuels for ramjet applications. Results indicate that not only is magnesium a desirable metal additive for fluorocarbon solid fuels, but boron can also be burned effectively with fluorocarbons. Kubota and Serizawa<sup>2</sup> performed detailed experimental work on the combustion of magnesium-based solid fuels containing magnesium, PTFE, and a small amount of Viton A. They observed that the burning rate of this type of solid fuel increases with increased magnesium content but decreases with increased particle size. The significance of the exothermic reactions immediately above the burning surface on the combustion process was also addressed.

Manser et al.<sup>3</sup> recently developed a number of highly energetic binders. In view of the large positive value of the heat of formation associated with poly(BAMO/NMMO), they claimed that a theoretical increase of the specific impulse by 5 s is possible when this polymer is used as a binder in a minimum-smoke propellant system. The total energy released from the fuel was found to increase significantly with the addition of percentages of boron to poly(BAMO/NMMO).

The major purpose of this paper is to study the fundamental ignition and combustion characteristics of Mg/PTFE/Viton A and boron/poly(BAMO/NMMO) solid fuels and to develop a convenient method for measuring the thermophysical properties of these two types of solid fuels. The specific objectives are

- 1) to determine the burning rates of both fuels as functions of pressure and ambient gas;
- 2) to characterize the ignition and combustion behavior by performing CO<sub>2</sub> laser ignition/combustion tests, x-ray diffrac-

Presented as Paper 88-3041 at the AIAA/ASME/SAE/ASEE 24th Joint Propulsion Conference, Boston, MA, July 11-13, 1988; received Aug. 22, 1988; revision received Sept. 16, 1989. Copyright © 1988 by the American Institute of Aeronautics and Astronautics, Inc. All rights reserved.

\*Associate Scientist, Chung-Shan Institute of Science & Technology, R.O.C.

†Assistant Professor, Department of Mechanical Engineering, Member AIAA.

‡Graduate Assistant, Department of Mechanical Engineering, Student Member AIAA.

§Associate Professor, Department of Mechanical Engineering, Member AIAA.

¶Distinguished Professor, Department of Mechanical Engineering, Associate Fellow AIAA.

tion analysis, low-pressure deflagration limit (PDL) tests, and microscopic examinations; and

3) to deduce the thermophysical properties from the measured subsurface temperature profiles (STP).

### Experimental Approach

A windowed strand burner and a CO<sub>2</sub> laser facility were used to study the ignition and combustion behavior of these two types of solid fuels and to characterize their thermophysical properties under well-controlled conditions. A brief description of the test facilities is given below, followed by a discussion of results obtained for each of the metal-based solid fuels.

#### Strand Burner

Figure 1 shows a schematic diagram of the windowed strand burner. A fuel sample (5 mm in diameter and 77 mm in length) was mounted vertically in the chamber. Ignition of the sample was achieved by passing an electrical current into a nichrome wire which pierced through the test sample about 3 mm from the top surface. A scale was optically superimposed on the image of the solid-fuel sample, using a 75 × 75 mm semitransparent mirror. To visualize the burning process, a video-recording system was employed to photograph the motion of the burning surface inside the strand burner and the optically superimposed scale. With this technique, the burning rate could be determined precisely from the length of the sample burned in a certain time duration. In addition to the visualization study, an imbedded fine-wire thermocouple (platinum/platinum-13% rhodium) with a diameter of 50 μm was used to measure the temperature profiles in both the subsurface and surface regions. A more detailed discussion of the overall strand burner system is given in Ref. 4.

The strand burner was used to study both the steady-state burning behavior and the PDL. During each steady firing, the chamber pressure was maintained at a prescribed level by means of a computer-controlled gas supply system. For the PDL tests, the chamber was depressurized at a rate of

1.1 kPa/s. The extinguishment point could then be identified from the measured pressure-time trace. After each test firing, the solid residues were collected for microscopic examination and x-ray diffraction analysis.

#### CO<sub>2</sub> Laser Ignition/Combustion Facility

A high-powered CO<sub>2</sub> laser (Coherent Super 48) capable of generating 800 W in continuous wave mode was used for the ignition and combustion studies. Figure 2 shows a schematic diagram of the facility. In order to generate a relatively uniform beam, a thin piece of sheet metal with a 7 mm-diam hole was used to allow only the most uniform portion of the laser beam to reach the sample surface. The resulting spatial variation of the beam intensity was  $\pm 10\%$ .<sup>5</sup> A test chamber (25 × 25 × 25 cm) was fabricated using 2.54-cm-thick plexiglass and a 1.25-cm-thick stainless steel top cover. The transparent nature of this chamber facilitated visual access to the ignition and combustion processes from all directions. Two high-quality glass windows were mounted on opposing sides of the chamber to allow for schlieren photography. A KCl window was installed in the top of the chamber to allow the laser to pass into the chamber when pressures other than atmospheric were needed.

A high-speed video system (Spin-Physics 2000) was used to record the dynamic behavior of the flame at a framing rate of 2000 pictures/s. The system accommodates two cameras capable of recording schlieren images and direct photographs simultaneously. The schlieren image can detect clearly the initiation of fuel gasification and its subsequent processes, whereas the direct photograph provides information about luminous flame development and burning characteristics.

In addition to its role in the ignition and combustion study, the CO<sub>2</sub> laser system was also used to conduct laser-flash tests for measuring the thermal diffusivities of the fuel samples. A 75-μm K-type (chromel/alumel) thermocouple was bonded to the bottom of the fuel sample having a specified thickness. As the laser flash irradiated the sample surface, the temperature detected by the bonded thermocouple was recorded by a Nicolet oscilloscope and could then be used to calculate the thermal diffusivity of the fuel.

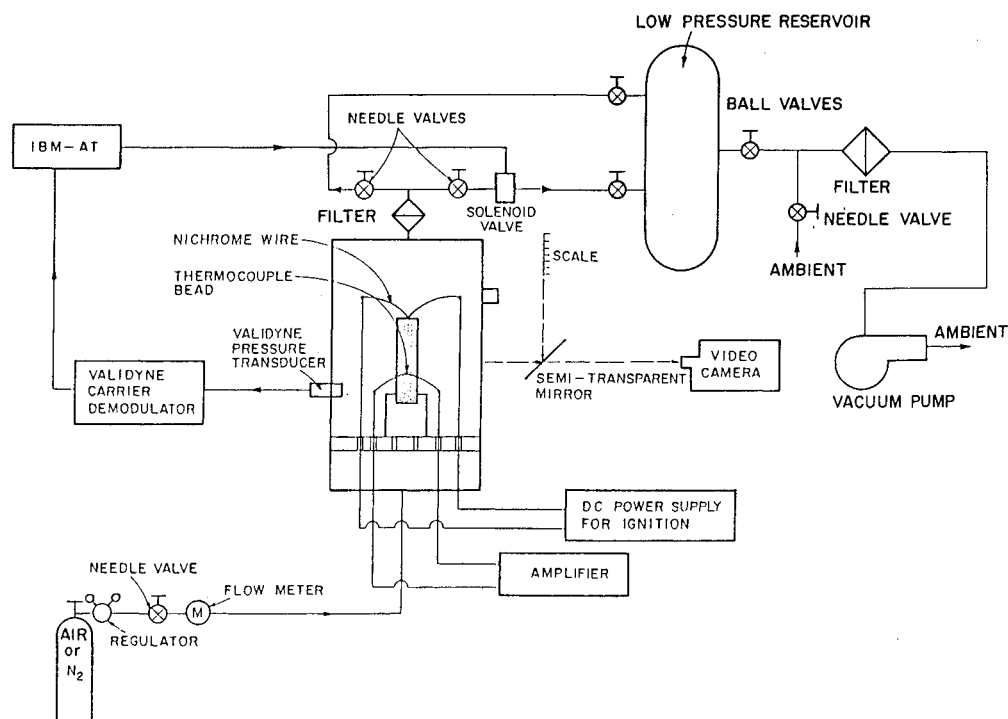


Fig. 1 Schematic of experimental apparatus used in strand-burner tests.

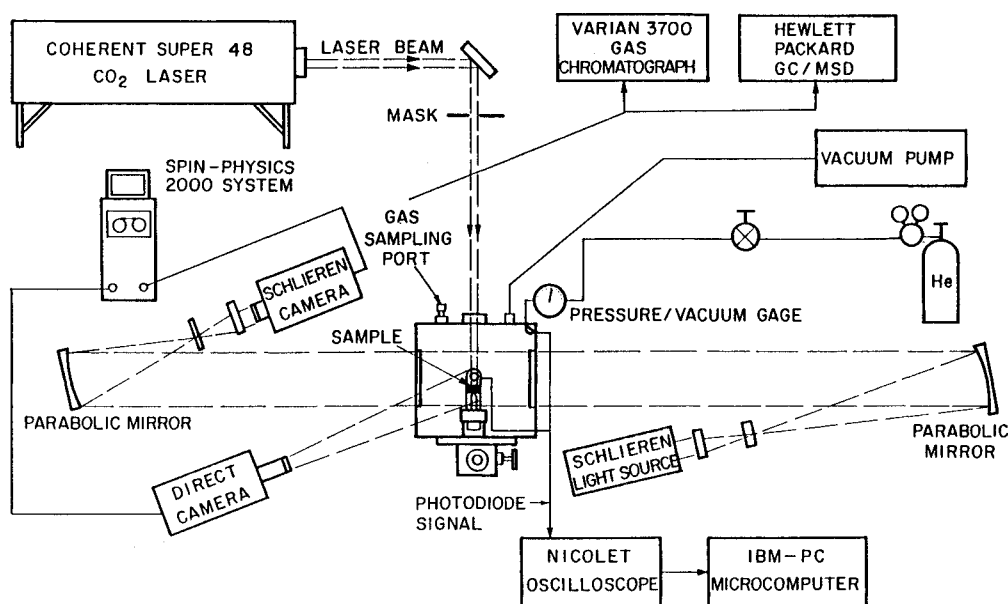


Fig. 2 Schematic of experimental apparatus used in CO<sub>2</sub> laser tests.

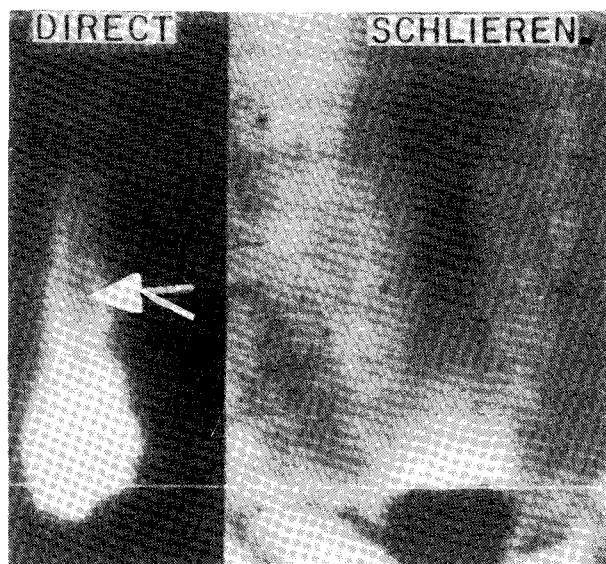


Fig. 3 Mg/PTFE/Viton A combustion in CO<sub>2</sub> laser test.

### Combustion Characteristics of Magnesium-Based and Boron-Based Solid Fuels

#### Magnesium-Based Solid Fuel

The magnesium-based solid fuels used in this study consisted of 50% fluorocarbons (PTFE and Viton A) and 50% magnesium powders with a mean diameter of 20  $\mu\text{m}$ . Initial tests were performed in the CO<sub>2</sub> laser facility, and subsequent experiments in the strand burner. In both cases, not only did the luminous flame initiate at the surface, but it remained attached to the surface for the duration of the combustion period. Figure 3 shows a typical flame structure of the fuel following ignition. The ejection of magnesium particles from the burning surface can be observed as indicated by the arrow in the direct image. This phenomenon was also noted in the strand-burning tests using both air and nitrogen. However, the height of the luminous flame was much greater for combustion tests performed in air than for those performed in nitrogen. The ignition delay time for the magnesium-based fuel was also determined for various oxygen percentages. It increased from 43 ms to 52 ms as the oxygen concentration increased from 1.0% to 21.0%, respectively. These tests were

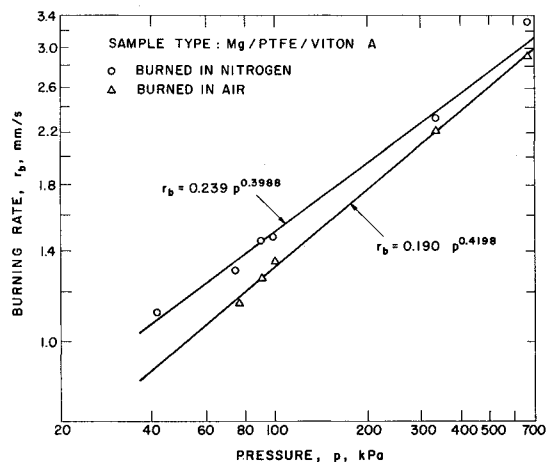


Fig. 4 Burning rate as a function of pressure for Mg/PTFE/Viton A in nitrogen and air.

performed at 100 kPa, with an incident heat flux of 400 W/cm<sup>2</sup> from the laser.

Figure 4 illustrates the dependence of the burning rate on the chamber pressure in two different gaseous environments. The burning rate was found to increase monotonically as the pressure increased, and to follow the Saint-Robert's law closely. It is interesting to note that despite the fuel-rich nature of the sample, the burning rate measured in nitrogen was consistently higher than that in air by approximately 10%. This observation is substantiated by the PDL results which show that the lowest pressures for sustaining stable combustion are 9.8 and 28.1 kPa for nitrogen and air, respectively. The fuel has a tendency to extinguish faster in air than in nitrogen. These results suggest that the burning characteristics of this type of solid fuel depend upon the composition of the ambient gas.

Figure 5 shows two temperature profiles obtained from 50- $\mu\text{m}$  thermocouples imbedded in the solid fuel. The tests were performed at atmospheric conditions in both air and nitrogen. Both curves indicate a surface temperature (characterized by the inflection point in the temperature profile) in the neighborhood of 850°C, but with different spatial distributions depending on the gas environment. The temperature profile in the vicinity of the surface is steeper when the fuel was burned in nitrogen, suggesting a higher heat-transfer rate at the surface.

Based upon the above observations, it is believed that the oxygen in the air has an adverse effect on the regression rate, ignition, and extinction characteristics of the solid fuel containing magnesium and fluorocarbons. A proposed rationale to explain this phenomenon follows.

First, the surface regression is a local phenomena. The regression rate is determined mainly by the highly exothermic gas-phase and heterogeneous reactions occurring immediately above and on the surface, and the thermal properties of the solid fuel which control the thermal wave propagation. The processes away from the surface play a less significant role due to their weak effect on the local heat transfer to the surface region.

Second, the magnesium-based solid fuel contained 50% magnesium, which is 17% greater than the stoichiometric ratio. Because of this, most of the magnesium powder did not burn completely in the near-surface region. Instead, the powder was ejected from the surface as a result of the expansion processes of gaseous products generated by the pyrolysis and the solid-phase reaction of the fluorocarbons surrounding them.

Third, the gaseous products originating from the surface act as a freejet and entrain the ambient gas into the shear layer surrounding the sample boundary. Thus, during tests in air, oxygen can be entrained easily, causing competitive oxidation and fluorination reactions with magnesium. Because the heat of oxidation for magnesium is approximately one-half of the heat of fluorination for magnesium, the total heat generated in the near-surface region is reduced when oxygen is present. This reduced heat release reduces the heat-transfer rate to the condensed phase and consequently decreases the regression rate.

This argument is substantiated by the subsurface temperature profiles measured in air and nitrogen environments (see

Fig. 5). Results based upon the x-ray diffraction analysis of the combustion residues indicate that the major solid products for the case involving air were  $\text{MgO}$ ,  $\text{MgF}_2$ , and carbon. However, for the pure nitrogen case, the major products were  $\text{MgF}_2$ ,  $\text{Mg}$ , and carbon. Thus, the reaction of magnesium particles with oxygen in the gas phase is significant. Further investigation is needed to quantify the extent to which the oxidation reaction takes place in the near-surface region.

Based upon the above observations and the measured subsurface temperature profiles, the important physicochemical processes involved in the combustion of magnesium/fluorocarbon fuel in the presence of air can be characterized qualitatively. Figure 6 summarizes the entire process by identifying five distinct regions in both the gas and condensed phases. A thermocouple trace obtained from a test in air at 100 kPa is also included to show the approximate thermal wave profile. These five zones can be summarized as follows.

In zone 1, the temperature is below the exothermic decomposition temperature of Viton A ( $316^\circ\text{C}$ ) and only inert heating takes place. Zone 2 covers a temperature range from  $316$ – $530^\circ\text{C}$ , corresponding to the decomposition temperatures of Viton A and PTFE, respectively. The thickness is about  $170\text{ }\mu\text{m}$  at 1 atm. Exothermic decomposition of Viton A initiates in this zone and reaches its maximum rate at  $471^\circ\text{C}$ .<sup>6</sup> The major products from the pyrolysis of Viton A include  $\text{HF}$ ,  $\text{C}_2\text{F}_2$ ,  $\text{C}_2\text{F}_4$ ,  $\text{CHF}_3$ , and other fluorocarbons and hydrofluorocarbons.<sup>6</sup> Chemical reactions between magnesium powders and the pyrolysis products of Viton A may also occur. Onset of the melting process of PTFE ( $330^\circ\text{C}$ ) occurs approximately  $200\text{ }\mu\text{m}$  beneath the burning surface. However, as a result of the highly viscous nature of the molten PTFE, only restricted motions of magnesium particles are possible in this region.

Zone 3 is characterized by a rapid temperature increase

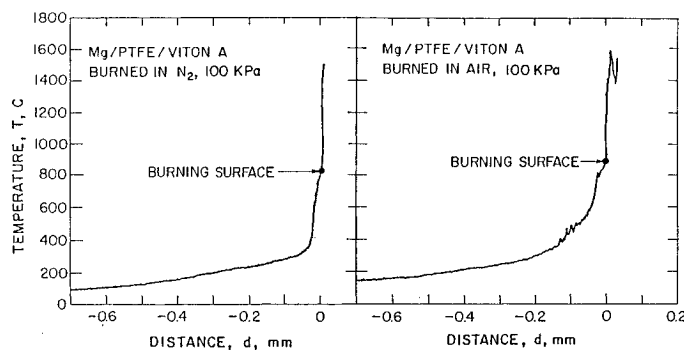


Fig. 5 Temperature profiles of Mg/PTFE/Viton A.

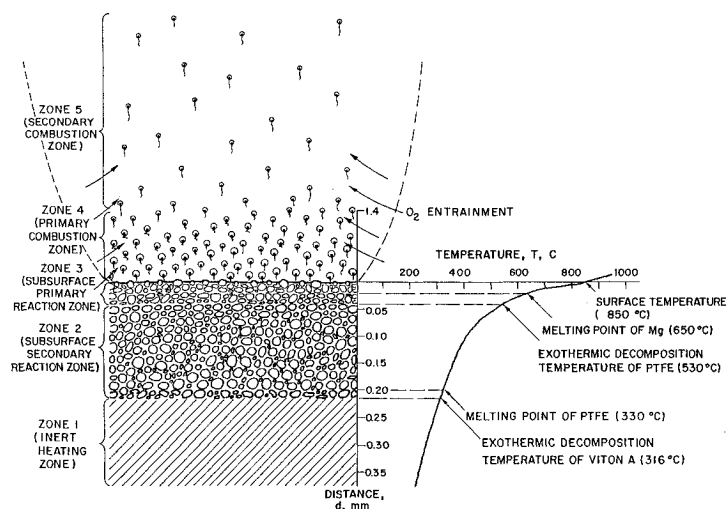


Fig. 6 Schematic showing temperature profile of subsurface region in a Mg/PTFE/Viton A sample.

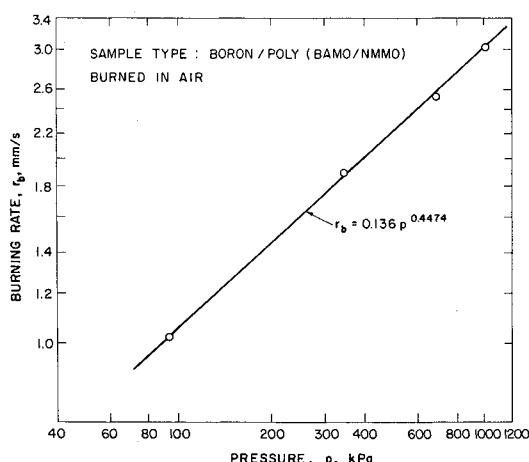


Fig. 7 Burning rate as a function of pressure for poly(BAMO/NMMO) with 17.6% boron.

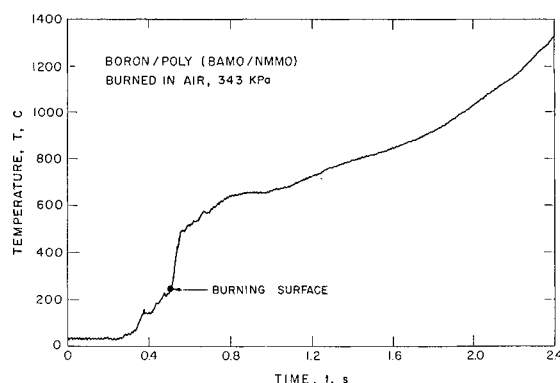


Fig. 8 Subsurface temperature profile of boron/poly(BAMO/NMMO) in air at 343 kPa.

within a thin layer of approximately  $50\text{ }\mu\text{m}$ . The temperature ranges from  $530^\circ\text{C}$  to the surface temperature of  $850^\circ\text{C}$ . At  $530^\circ\text{C}$ , PTFE begins to decompose exothermically to liberate  $\text{CF}_4$ ,  $\text{C}_2\text{F}_6$ ,  $\text{C}_2\text{F}_4$ ,  $\text{C}_3\text{F}_8$ ,  $\text{C}_4\text{F}_{10}$ , other fluorocarbons, and possibly fluorine itself.<sup>6</sup> As the temperature further increases to  $650^\circ\text{C}$ , magnesium powders begin to melt. Reactions that may take place in this region are believed to be those of fluorine and fluorinated compounds with either liquid or gaseous magnesium (because the vapor pressure of magnesium at  $850^\circ\text{C}$  is about  $50\text{ mm Hg}$ ). These highly exothermic reactions may further enhance the gasification of PTFE, causing an imbalance of local forces. This process results in violent expulsion of magnesium particles from the surface.

Zone 4 is characterized by the high-temperature gradient in the vicinity of the burning surface. It is depicted by a bright flame associated with the exothermic gas-phase and heterogeneous reactions. As stated above, for combustion in air, oxygen may be entrained by the jet and react with molten magnesium powders near the outer region of the surface.

Zone 5 is rather far from the surface. For combustion in air, the major chemical process includes the reaction of magnesium vapor and  $\text{O}_2$ . As a result of its distance from the surface and its low flame temperature ( $\sim 1600^\circ\text{C}$ ),<sup>7</sup> the effects of this region on surface-regression processes are insignificant.

#### Boron/Poly(BAMO/NMMO) Solid Fuel

In this work, the boron-based solid fuel sample contained a highly energetic copolymer, BAMO/NMMO, and 17.6% boron powder with a mean diameter of  $0.5\text{ }\mu\text{m}$ . From the recorded video images, it was observed that the flame structure of the sample was affected by the testing pressure. At atmospheric conditions, only a faint gaseous flame appeared

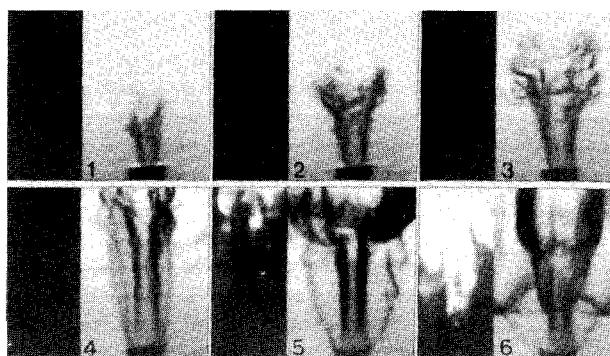


Fig. 9 Ignition sequence of pure poly(BAMO/NMMO) in air with a heat flux of  $190\text{ W/cm}^2$  using  $\text{CO}_2$  laser. Time from initial laser heating is 4.5, 5.5, 6.5, 88.0, 128.0, and 165.5 ms.

above the surface. As the ambient pressure was increased to  $1034\text{ kPa}$ , a much brighter flame was observed, with many burning boron particles ejected from the surface.

Figure 7 shows the strand-burning rate in air as a function of pressure. It followed the Saint-Robert's law with the burning rate given by  $r_b = 0.136 p^{0.447}$ . Figure 8 presents a measured temperature profile obtained, using a  $50\text{ }\mu\text{m}$  R-type thermocouple embedded in a boron/poly(BAMO/NMMO) sample, with an ambient pressure of  $343\text{ kPa}$ . The burning-surface temperature, indicated by a sudden temperature jump at the burning surface, was about  $250^\circ\text{C}$ , which was relatively low when compared to magnesium-based solid fuels. The burning-surface temperature increased monotonically with testing pressure, ranging from  $220^\circ\text{C}$  at  $100\text{ kPa}$  to  $310^\circ\text{C}$  at  $1030\text{ kPa}$ . The temperature-time trace presented in Fig. 8 shows several ripples between  $100^\circ\text{C}$  and  $250^\circ\text{C}$ ; these are believed to be caused by the subsurface reaction of the binder.<sup>8-10</sup> In this particular test, the maximum measured gas-phase temperature was about  $1400^\circ\text{C}$ . However, in some tests, the measured temperature-time traces showed maximum temperatures higher than  $1715^\circ\text{C}$ .

To further enhance understanding of the ignition and combustion behavior, the boron-based fuel samples were also tested in the  $\text{CO}_2$  laser facility. Figure 9 shows an ignition sequence of the pure poly(BAMO/NMMO) under  $\text{CO}_2$  laser heating. The left image is a direct picture, and the right image is a schlieren picture. The magnification of the direct image is twice that of the schlieren, and the sample is a  $5\text{ mm}$  cube.

Pyrolysis of the solid fuel was first noted after  $4.0\text{ ms}$  in the schlieren picture. The gases formed a jet with a mean velocity of about  $10\text{ m/s}$ . Within a distance of  $8\text{ mm}$  from the surface, the jet appeared to be laminar in nature and became turbulent farther away from the surface. The gases gradually absorbed the incident laser energy and finally ignited after  $128\text{ ms}$ . This ignition process is evident in the direct picture and is an indication of a gas-phase ignition process. Immediately following ignition, the flame propagated down toward the surface to further enhance the condensed phase reactions. The copolymer extinguished following laser cutoff at  $200\text{ ms}$ .

Figure 10 shows the ignition process of poly(BAMO/NMMO) containing 17.6% boron. Gasification was noted at  $4.5\text{ ms}$  after onset of the  $\text{CO}_2$  laser beam. The pyrolyzed gaseous jet was less turbulent than that evolved from the pure poly(BAMO/NMMO) sample. Changes in the jet characteristics are believed to be dependent upon the boron content in the sample which acts to dampen the turbulent mixing process.<sup>11</sup> Because the boron is initially ejected before burning, the solid boron particles in the gas phase absorb the incident laser energy, thus raising the temperature in the gas phase to initiate chemical reaction and lead to ignition. The increase of absorption due to the presence of boron in the gas phase has been verified by laser-attenuation tests with various gases and solid-fuel samples.<sup>5</sup> As a result, the boron addition decreases

the ignition delay time to 10 ms, compared to 128 ms for the pure poly(BAMO/NMMO).

Picture 6 in Fig. 10 shows many boron particles burning in the gas phase following ignition. After laser cutoff, the sample extinguished momentarily and then reignited. The reignition, which was observed for the boron-containing fuels but not for the pure copolymer, is believed to be the result of an increase in thermal diffusivity caused by the boron addition, which allows the thermal wave to penetrate further into the solid fuel.

Figure 11 shows the ignition delay times for pure poly(BAMO/NMMO) and samples containing 17.6 and 30% boron as a function of heat flux. The pure poly(BAMO/NMMO) fuel exhibited random ignition characteristics for all heat fluxes. When boron was added, the delay time became shorter and reproducible. The behavior of boron/poly(BAMO/NMMO) is distinctly different from that of pure poly(BAMO/NMMO) due to the effects of boron particles on the fluid dynamics and radiative absorption. In the pure poly(BAMO/NMMO) case, the high turbulence level in the gas phase caused the pyrolyzed gases to be heated more uniformly; thus, no local high-temperature region could be established easily in the gas phase.

On the other hand, when boron is added, the gas phase becomes less turbulent due to the damping effect of submicron boron particles present in the pyrolyzed gases. This introduces a smaller heat-transfer rate within the pyrolyzed gases and causes a local high-temperature region to be established more readily. In addition, the radiative absorption by the pyrolyzed gases mixed with boron particles is significantly increased. The ignition delay time of boron/poly(BAMO/NMMO) is, therefore, much shorter than that of pure poly(BAMO/NMMO).

### Thermophysical Property Characterization

Both subsurface temperature profile (STP) and laser-flash methods were used to evaluate the thermal diffusivities and conductivities of the fuel samples. Other properties, such as densities and specific heats, were obtained from the open literature. A brief description of these two measurement techniques is given below, followed by a discussion of results.

#### Subsurface Temperature Profile (STP) Method

In order to obtain a temperature profile of the subsurface region during combustion, an R-type fine-wire thermocouple with a diameter of 50  $\mu\text{m}$  was embedded in a vertically mounted solid fuel sample. The sample was then ignited using a nichrome wire and burned down into the imbedded thermocouple. In this manner, both the subsurface and gas-phase temperature profiles were obtained. The subsurface temperature profile could be used to deduce the thermal diffusivity and conductivity as functions of temperature.

The STP method is based upon a one-dimensional heat-conduction equation. In order to simplify the analysis, a moving coordinate system was used with its origin located at

the instantaneous burning surface. Using this coordinate system, the heat-conduction equation becomes<sup>12,13</sup>

$$\frac{d}{dx} K \frac{dT}{dx} - \frac{d(\rho_p r_b C_p T)}{dx} + \rho_p \dot{q}_{sub} = 0 \quad (1)$$

where  $\dot{q}_{sub}$  is the net heat release in the subsurface region of the fuel sample. This term vanishes if there is no chemical reaction within this region (i.e., the inert heating region).

Integration of Eq. (1) gives

$$K \frac{dT}{dx} \Big|_x - K \frac{dT}{dx} \Big|_{-\infty} = \int_{-\infty}^x \frac{d(\rho_p r_b C_p T)}{dx} dx \\ = \int_{T(-\infty)}^{T(x)} \rho_p r_b C_p dT \quad (2)$$

The density and specific heat are evaluated using a mass-averaged value of the ingredients in the solid fuel sample. Rearranging Eq. (2) and assuming that the heat flux is zero at  $x = -\infty$ , the thermal conductivity as a function of temperature becomes

$$K(T) = \int_{T(-\infty)}^{T(x)} \rho_p r_b C_p dT \Big/ \left. \frac{dT}{dx} \right|_x \quad (3)$$

where the local temperature gradient  $dT/dx$  can be calculated from the measured subsurface temperature profile. By definition, the thermal diffusivity can be deduced from the relation

$$\alpha(T) = K/(\rho_p C_p) \quad (4)$$

Because the STP method was used to deduce the thermal conductivity and diffusivity of the testing sample in the inert region, the thermocouple bead did not experience rapid temperature variations and thus was able to measure the temperature profile very accurately. The characteristic time of the thermocouple used in this study was about 10 ms,<sup>14</sup> which is much smaller than heat-conduction time within the inert region. Measurement errors caused by velocity and radiation effects<sup>15</sup> are not present since the thermocouple is embedded in a solid, opaque fuel sample. Because of the small diameter of the thermocouple wire, heat losses caused by conduction from the thermocouple bead are also negligible.<sup>15</sup> The largest error introduced into the STP method ( $\pm 10^\circ\text{C}$ ) comes from the data acquisition and reduction procedures.

#### Laser-Flash Method

The laser-flash method<sup>16</sup> was also used to determine the thermal diffusivity of the solid fuel samples. In this method, a short laser pulse was given to the top surface of the sample. A thermocouple was mounted to the bottom surface of the

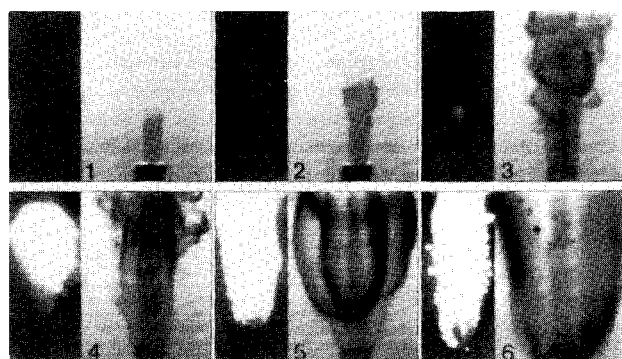


Fig. 10 Ignition sequence of poly(BAMO/NMMO) with 17.6% boron in air with a heat flux of 490  $\text{W}/\text{cm}^2$  using  $\text{CO}_2$  laser. Time from initial laser heating is 5.0, 6.0, 10.0, 17.5, 42.0, and 140.5 ms.

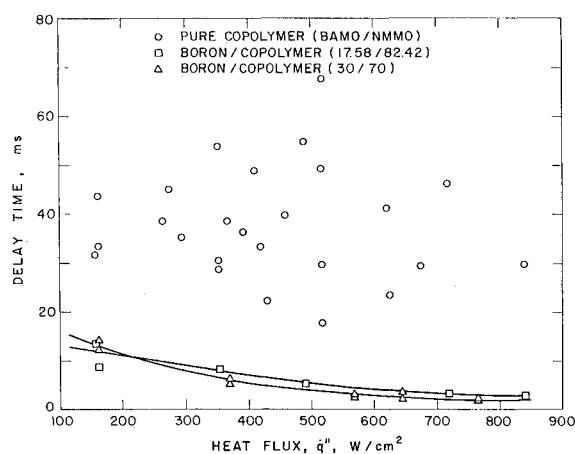


Fig. 11 Ignition delay time vs heat flux for pure poly(BAMO/NMMO) binder.

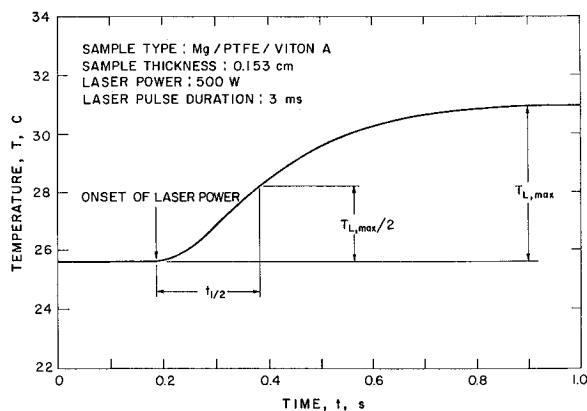


Fig. 12 Temperature-time trace from laser-flash test.

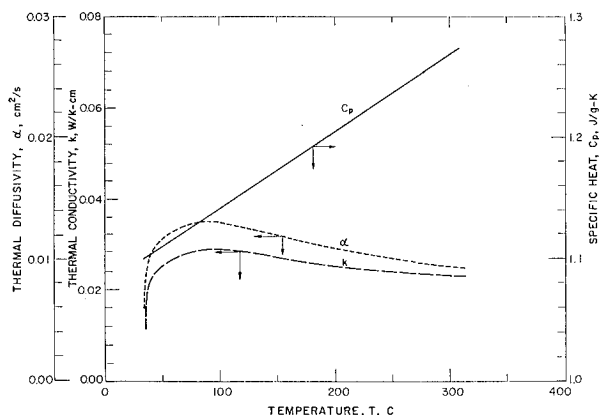


Fig. 13 Thermophysical properties of Mg/PTFE/Viton A as functions of temperature from STP method.

sample to monitor the temperature rise as the energy from the top surface was conducted through the sample (thickness of 1 mm). Figure 12 shows a typical temperature-time trace from the thermocouple on the bottom surface. The temperature rises slowly and reaches a maximum value ( $T_{L,max}$ ) after 800 ms.

If we assume that the solid fuel sample has a uniform initial temperature distribution and that the energy from the laser pulse is instantaneously and uniformly absorbed in a thin layer on the top surface, then the temperature rise on the bottom face can be expressed as<sup>17</sup>

$$T(L,t) = T_{L,max} \left[ 1 + \frac{1}{2} \sum_{n=1}^{\infty} (-1)^n \exp\left(-\frac{n^2 \pi^2}{L^2} \alpha t\right) \right] \quad (5)$$

When  $T(L,t)/T_{L,max} = 1/2$ , the dimensionless quantity  $\pi^2 \alpha t / L^2$  must have a value of 1.37. Consequently, the thermal diffusivity becomes

$$\alpha = \frac{1.37 L^2}{\pi^2 t_{1/2}} = \frac{0.139 L^2}{t_{1/2}} \quad (6)$$

where  $t_{1/2}$  is the time required for the bottom face to attain one-half of its maximum temperature. Equation (6) is accurate within 1% as long as the laser-pulse length is short enough to avoid any chemical reactions and the characteristic time of the sample (defined as  $t_c = L^2 / \pi^2 \alpha$ ) is greater than 50 times the laser-pulse duration.<sup>18</sup> The characteristic time and the pulse duration thus determine the thickness of the solid fuel sample.

Heat losses by convection from the top surface during the laser-flash method was investigated by Mendelsohn.<sup>19</sup> He found that the heat loss by convection depends strongly upon

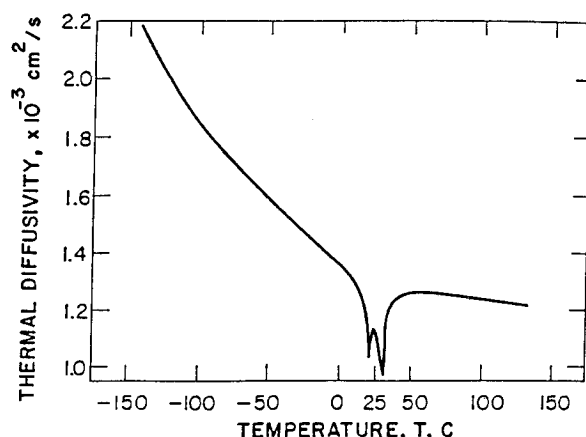


Fig. 14 Thermal diffusivity of PTFE between -140 and 125°C.<sup>23</sup>

the testing conditions, sample properties, and the Biot number. In order to minimize heat losses, the Biot number for the tests conducted in this study were of the order of 0.02, ensuring the reliability of the data. In addition, the sample was mounted on insulation material to minimize conductive losses from the bottom surface.

### Thermophysical Properties of Magnesium-Based and Boron-Based Solid Fuels

Figure 13 shows the results obtained by the STP method for the magnesium-based solid fuel. The specific heat, thermal conductivity, and thermal diffusivity are plotted as functions of temperature. The specific heat and density of Mg, PTFE, and Viton A were obtained from Refs. 20–22, respectively. At a temperature of about 40°C, the values for both thermal conductivity and thermal diffusivity increase drastically. This sharp increase is believed to be caused by the rapid change in thermal diffusivity of PTFE that occurs near that temperature due to the crystalline transition (see Fig. 14).

To verify the measurements with the STP method, the laser-flash method was used to determine the thermal diffusivity of the magnesium-based solid fuel at 25°C. Using a sample thickness of 0.153 cm, a value of  $1.6 \times 10^{-2} \text{ cm}^2/\text{s}$  was measured; this agrees reasonably well with the value of  $1.1 \times 10^{-2} \text{ cm}^2/\text{s}$  obtained using the STP method. The laser-flash method was also used to determine the thermal diffusivity of boron/poly(BAMO/NMMO) solid fuel, and a value of  $1.82 \times 10^{-3} \text{ cm}^2/\text{s}$  was obtained at 25°C. Temperature profiles were measured for the boron/poly(BAMO/NMMO) fuel; however, the thermal diffusivity could not be calculated because the specific heat and density are not known.

### Summary and Conclusions

The combustion behavior and thermophysical properties of magnesium-based and boron-based solid fuels have been studied using both a windowed strand burner and a CO<sub>2</sub> laser test facility. Results from strand-burner tests show that the magnesium-based fuel burns 10% faster in nitrogen than in air, indicating that oxygen has an adverse effect on the combustion behavior of this type of fuel. To verify the oxygen effect, ignition delay times were measured using different oxygen percentages. It was found that the ignition delay time decreased as the oxygen percentage decreased. PDL tests show that the fuel has a low pressure limit of 9.8 kPa for stable combustion in nitrogen, compared to 28.1 kPa in air. Subsurface temperature profiles of the magnesium-based fuel also indicate the adverse effect of oxygen on the combustion behavior.

The combustion behavior of the boron-based solid fuel was also studied in the strand burner, and its burning rate was found to have a slightly higher pressure dependence than that

for the magnesium-based solid fuel. Expressions for the burning rate of the magnesium-based fuel in air, in nitrogen, and for the boron-based fuel in air were found to be  $0.190 p^{0.42}$ ,  $0.239 p^{0.40}$ , and  $0.136 p^{0.45}$ , respectively. To investigate the effect of boron on the pure poly(BAMO/NMMO) energetic binder, ignition delay times were studied. Results showed that the random ignition delay times for the pure poly(BAMO/NMMO) became consistent when boron was added. From high-speed pictures of the ignition process, it was found that the boron particles affect the fluid dynamics for the gaseous jet. The boron also resulted in increased absorptivity in the gas phase. The combined result is a significant decrease in the ignition delay time.

An STP method was developed in order to determine the thermophysical properties as functions of temperature for these fuels, and the results were compared with those of a laser-flash method. Knowing the value for the specific heat of magnesium-based solid fuel as a function of temperature, the thermal conductivity and thermal diffusivity of the fuel were calculated from a subsurface temperature-time trace. The agreement of these two methods demonstrates the validity of the STP method.

### Acknowledgments

This work represents a part of the research results obtained under Contract N00014-86-K-0468 sponsored by the Office of Naval Research, Arlington, VA, under the management of R. S. Miller and G. D. ROY. The authors would like to thank R. G. Shortridge of the Naval Weapon Supply Center and G. E. Manser of Aerojet Solid Propulsion Company for providing the solid fuels used in this study. The assistance of B. L. Fetherolf of The Pennsylvania State University is greatly appreciated in performing the CO<sub>2</sub> laser-ignition tests.

### References

- <sup>1</sup>Peretz, A., "Some Theoretical Considerations of Metal-Fluorocarbon Compositions for Ramjet Fuels," *8th International Symposium on Air-Breathing Engines*, AIAA, New York, 1987, pp. 398-403.
- <sup>2</sup>Kubota, N., and Serizawa, C., "Combustion of Magnesium/Polytetrafluoroethylene," *AIAA* 86-1592, 1986.
- <sup>3</sup>Manser, G. E., Fletcher, R. W., and Knight, M. R., "High Energy Binders," Final Rept., Thiokol Corp., Brigham City, UT, Contract N00014-82-C-0800, June 1985.
- <sup>4</sup>Hsieh, W. H., "Study of Strand and Erosive Burning of NOSOL-363 Stick Propellants," Ph.D. Thesis, The Pennsylvania State Univ., University Park, PA, 1987.
- <sup>5</sup>Fetherolf, B. L., Litzinger, T. A., and Kuo, K. K., "An Instrument for Measuring High-Power Laser Beam Profiles and Beam Attenuations," *The Review of Scientific Instruments*, Vol. 61, No. 1, 1990, pp. 7-10.
- <sup>6</sup>Chen, D. M., Fetherolf, B. L., Snyder, T. S., Hsieh, W. H., Litzinger, T. A., and Kuo, K. K., "Ignition and Combustion Behavior of MTV Igniter Materials for Base Bleed Application," *First International Symposium on Special Topics in Chemical Propulsion: Base Bleed*, Athens, Greece, Nov. 23-25, 1988, Hemisphere, New York (to be published).
- <sup>7</sup>Newman, R. N., and Payne, J. F. B., "The Anomalous Brightness of Magnesium-Air Flames," *Combustion and Flame*, Vol. 68, No. 1, 1987, pp. 31-41.
- <sup>8</sup>Farber, M., Harris, S. P., and Srivastava, R. D., "Mass Spectrometric Kinetic Studies on Several Azido Polymers," *Combustion and Flame*, Vol. 55, No. 2, 1984, pp. 203-211.
- <sup>9</sup>Oyumi, Y., and Brill, T. B., "Thermal Decomposition of Energetic Materials 14. Selective Product Distributions Evidenced in Rapid, Real-Time Thermolysis of Nitrate Ester at Various Pressures," *Combustion and Flame*, Vol. 66, No. 1, 1986, pp. 9-16.
- <sup>10</sup>Oyumi, Y., and Brill, T. B., "Thermal Decomposition of Energetic Materials 12. Infrared Spectral and Rapid Thermolysis Studies of Azido-Containing Monomers and Polymers," *Combustion and Flame*, Vol. 65, No. 2, 1986, pp. 127-135.
- <sup>11</sup>Snyder, T. S., Chen, D. M., Fetherolf, B. L., Litzinger, T. A., and Kuo, K. K., "Pyrolysis and Ignition of Boron-Based Solid Fuels for Ramjet Applications," *25th JANNAF Combustion Meeting*, Huntsville, AL, CIA Pub. 498, 1988.
- <sup>12</sup>Klein, R., Mentser, M., Von Elbe, G., and Lewis, B., "Determination of the Thermal Wave Structure of a Combustion Wave by Fine Thermocouples," *Journal of Physics and Colloid Chemistry*, Vol. 54, No. 6, 1950, pp. 877-884.
- <sup>13</sup>Kubota, N., Ohlemiller, T. J., Caveny, L. H., and Summerfield, M., "The Mechanisms of Super-Rate Burning of Catalyzed Double Base Propellants," Dept. of Aerospace and Mechanical Sciences, Rept. 1087, Princeton Univ. Princeton, NJ, March 1973.
- <sup>14</sup>Liperi, M., "Analisi Sperimentale Mediante Microtermocoppie Della Combustion Di Propellanti Solidi Con Proprieta Termiche Variabili," Tesi di Laurea, Dipartimento di Euretico, Politecnico di Milano, 1986.
- <sup>15</sup>Doebelin, E. O., *Measurement System, Application and Design*, McGraw-Hill, New York, 1975, Chap. 8.
- <sup>16</sup>Parker, W. J., Jenkins, R. J., Butler, C. P., and Abbott, G. L., "Flash Method of Determining Thermal Diffusivity, Heat Capacity, and Thermal Conductivity," *Journal of Applied Physics*, Vol. 32, No. 9, 1961, pp. 1679-1683.
- <sup>17</sup>Carslaw, H. S., and Jaeger, J. C., *Conduction of Heat in Solids*, 2nd Ed., Oxford Univ. Press, Oxford UK, 1959, pp. 92-101.
- <sup>18</sup>Taylor, R. E., and Cape, J. A., "Finite Pulse-Time Effects in the Flash Diffusivity Technique," *Applied Physics Letters*, Vol. 5, No. 10, 1964, pp. 212-213.
- <sup>19</sup>Mendelsohn, A. R., "The Effect of Heat Loss on the Flash Method of Determining Thermal Diffusivity," *Applied Physics Letters*, Vol. 2, No. 1, Jan. 1963, pp. 19-21.
- <sup>20</sup>Chase, M. W., Jr., Davis, C. A., Downey, J. R., Jr., Frurip, D. J., McDonald, R. A., and Syverud, A. N., "JANNAF Thermochemical Tables," 3rd ed., *Journal of Physical and Chemical Reference Data*, Vol. 14 (Suppl.), No. 1, 1985, pp. 1462-1466.
- <sup>21</sup>Marx, P., and Dole, M., "Specific Heat of Synthetic High Polymers. V. A Study of the Order-Disorder Transition in PTFE," *Journal of the American Chemical Society*, Vol. 77, Sept. 20, 1955, pp. 4771-4774.
- <sup>22</sup>DuPont Technical Personnel, private communication, June 1988.
- <sup>23</sup>Shelley, D. L., and Huber, S. F., "Thermal Diffusivity of Poly(tetrafluoroethylene) between -140° and 125°C," *8th Heat Conductivity Conference*, 1972, pp. 1067-1077.